Assessment of stress-strain model for UHPC confined by steel tube stub columns

An Le Hoang[*1,2,3] and Ekkehard Fehling[3a]

[1]*Division of Construction Computation, Institute for Computational Science, Ton Duc Thang University, Ho Chi Minh City, Vietnam*
[2]*Faculty of Civil Engineering, Ton Duc Thang University, Ho Chi Minh City, Vietnam*
[3]*Faculty of Civil and Environmental Engineering, Institute of Structural Engineering, University of Kassel,
Kurt-Wolters-Strasse 3, 34125, Kassel, Germany*

Abstract. Ultra high performance concrete (UHPC) has recently been applied as an alternative to conventional concrete in construction due to its extremely high compressive and tensile strength, and enhanced durability. However, up to date, there has been insufficient information regarding the confinement behavior of UHPC columns. Therefore, this study aims to perform an assessment of axial stress-strain model for UHPC confined by circular steel tube stub columns. The equations for calculating the confined peak stress and its corresponding strain of confined concrete in existing models suggested by Johansson (2002), Sakino *et al.* (2004), Han *et al.* (2005), Hatzigeorgiou (2008) were modified based on the regression analysis of test results in Schneider (2006) in order to increase the prediction accuracy for the case of confined UHPC. Furthermore, a new axial stress-strain model for confined UHPC was developed. To examine the suitability of the modified models and the proposed model for confined UHPC, axial stress-strain curves derived from the proposed models were compared with those obtained from previous test results. After validating the proposed model, an extensive parametric study was undertaken to investigate the effects of diameter-to-thickness ratio, steel yield strength and concrete compressive strength on the complete axial stress-strain curves, the strength and strain enhancement of UHPC confined by circular steel tube stub columns.

Keywords: UHPC; confined concrete; steel tube; axial stress-strain model; confinement

1. Introduction

Due to remarkable advancement of concrete technology, ultra high performance concrete (UHPC) has recently received a great deal of attention for its practical applications in construction throughout the world. This is attributed to the fact that UHPC exhibits exceptional properties such as its extremely high compressive strength exceeding 150 MPa (about three to five times the strength of ordinary concrete) and sustained post-cracking tensile strength above 5 MPa, superior durability and very high energy absorption capacity (Fehling *et al.* 2014, Graybeal 2005). However, the use of UHPC for structural member under compression poses difficulties because of its inherent brittleness accompanying with higher compressive strength. As stated by current studies, the compressive ductility of UHPC is not well improved by incorporation of steel fibers even with increasing volume up to 2% (Yan and Feng 2008, Liu *et al.* 2012). Thus, to ensure the minimum ductility, some methods for confining UHPC column by combining it with steel reinforcements, or fiber reinforced polymer (FRP) tubes, or steel tubes have to be considered. Zohrevand and Mirmiran (2011) tested sixteen UHPC stub

columns confined by circular FRP tubes. The FRP confinement was found to significantly enhance both the ultimate strength and strain of UHPC. Similarly, Guler (2014) reported the results of 36 different types of FRP-wrapped circular UHPC short columns and pointed out that there was an average increase of 48% and 128% in the ultimate strength and strain, respectively, with the use of Carbon-FRP (CFRP) and Glass-FRP (GFRP). Recently, Yang *et al.* (2016) has presented an experimental study of the stress-strain behavior of circular UHPC stub columns confined by conventional transverse steel reinforcement. The test results of this study indicated that the confinement effect from steel reinforcement results in a larger ultimate strain than FRP confined UHPC at the same confinement ratio. The effect of the confining stress on the axial load response of square UHPC columns confined by transverse steel reinforcement was also investigated by several studies, such as Shin *et al.* (2016), Hosinieh *et al.* (2015), Empelmann *et al.* (2008), in which a more ductile failure mode of UHPC can be achieved by the combination of transverse steel reinforcements and steel microfibers. In addition to the confining method using FRP or steel reinforcement for UHPC columns, circular steel tube is found to be a suitable material which can generate an effective confinement owing to the continuous wrapping around UHPC columns and the optimum shape induced by the circular section (Susantha *et al.* 2001, Yang *et al.* 2016).

Moreover, numerous structural benefits can be offered by concrete filled steel tube columns (CFSTCs), including

*Corresponding author, Ph.D. Student
E-mail: lehoangan@tdt.edu.vn
[a]Professor
E-mail: fehling@uni-kassel.de

higher strength and stiffness, improved ductility, higher fire resistance and larger energy absorption capacities as compared to conventional steel reinforced concrete columns or steel structures (Han *et al.* 2014, Morino 2001). Besides, the steel tube works as a permanent formwork for casting concrete, thus leading to a reduction in the construction cost and time (Han *et al.* 2012). Therefore, CFSTCs have been widely applied in multi-storey bulding, bridge piers, and supporting structures, especially in some constructions for seismically active regions (Liew *et al.* 2010). For developing CFSTCs using ultra high strength material which can result in smaller column size and greater loading capacity, several researchers have studied on circular UHPC filled steel tube stub columns (UHPC-FSTCs). Guler *et al.* (2013), Yan and Feng (2008) stated that, for circular UHPC-FSTCs under uniaxial loading on both steel and concrete section, there is very little confinement effect provided by the steel tube to the UHPC core up to the peak load, while the ductility of circular UHPC-FSTCs after the peak load can be significantly improved when using thicker steel tube thickness. This conclusion was also drawn in the studies conducted by Liew *et al.* (2014, 2015, 2016), Liew and Xiong (2010, 2012), Xiong (2012), Tue *et al.* (2004a) and Schneider (2006). For this loading pattern, these authors explained that the Poisson's ratio of UHPC is smaller than that of steel tube in the elastic portion due to inherently small lateral deformation of UHPC and UHPC core is crushed before the yielding of steel tube, thereby causing no noticeable confinement effect which can be developed before reaching the peak load. However, it is asserted that, for UHPC-FSTCs, the tri-axial confinement effect become to be maximum when the load is imposed on only concrete core, thereby leading to a significant enhancement of both strength and ductility (Liew and Xiong 2012, An *et al.* 2016). Likewise, Tue *et al.* (2004b), Schneider (2006) proposed some practical possibilities of UHPC-FSTCs in buildings and bridges through a series of experiments on the compressive behavior of these columns using UHPC with compressive strengths ranging between 150 and 180 MPa. Based on the observations from the test results, these authors also accepted the notion that, for UHPC-FSTCs, the sufficient confinement by the steel tube can be achieved by applying the load only on the concrete cross section, thus restricting an abrupt load drop of UHPC core and enabling a more ductile failure of columns. From these findings, it can be argued that to obtain more benefits of both strength and ductility for CFSTCs using UHPC, the case of loading on concrete section should be further considered and examined.

From the survey of the authors, experimental and analytical studies on UHPC-FSTCs, in general, and on UHPC-FSTCs under loading on concrete core, in particular, remain very limited with only a handful of existing studies as discussed above. With respect to UHPC-FSTCs under loading on concrete core, to the best knowledge of the authors, apart from seven axial compression test specimens reported in Tue *et al.* (2004a), Schneider (2006), and two axial compression test specimens presented by Liew and Xiong (2012), Xiong (2012), there have been no such experimental studies up to present. Hence, additional studies to better understand the compressive behavior of this column type are requisite.

In the past, the majority of published experimental studies on circular CFSTCs under loading on concrete core were concerned with the use of normal strength concrete (NSC) or high strength concrete (HSC) (e.g., Johansson 2002, Liu *et al.* 2009, De Oliveira *et al.* 2010, Huang *et al.* 2012). According to Aboutaha and Machado (1998), Yu *et al.* (2010), for CFSTCs, when the column strength and ductility are considered as the most crucial factors in design, the load is suggested to be applied to only the concrete core. This loading pattern is often referred to as a form of steel tube confined concrete (STCC) columns, where the steel tube is mainly used to provide a lateral confining pressure to the concrete core and to prevent the shear failures in short columns rather than to provide a resistance to the axial stresses (Sun 2008). It is obvious that the most fundamental requirement in understanding the mechanical behavior of STCC columns is the knowledge of stress-strain curve of the confined concrete, thereby quantifying the strength and ductility enhancement arising from the confinement effect. Consequently, a considerable amount of research has been directed towards proposing the stress-strain relationships for concrete confined by circular steel tube.

Susantha *et al.* (2001) assumed a stress-strain model for concrete confined by circular steel tube with consideration of the change in the Poisson's ratio of both concrete and steel based on the method proposed by Tang *et al.* (1996). Han *et al.* (2005) presented a typical stress-strain curve for confined concrete in CFSTCs by the introduction of the confinement factor which representing the composite action between the concrete core and the steel tube. Likewise, Sakino *et al.* (2004), Hatzigeorgiou (2008) developed a stress-strain relationship for concrete core in CFSTCs through an evaluation of the confining effect on the increase in concrete strength obtained from the test results and empirical expressions. Based on the stress-strain curves of 18 test specimens of circular STCC stub columns, O'Shea and Bridge (2000) modified equations for predicting the confining pressure, the peak confined concrete strength and corresponding strain in two cases of concrete classifications including medium strength concrete up to 50 MPa and high strength concrete up to 100 MPa. Subsequently, Johansson (2002) evaluated the efficiency of passive confinement through a proposed stress-strain model for confined concrete with taking into account a volumetric strain history characterized by the level of applied confining stress, and then verified this model with test results of circular STCC stub columns using concrete strength up to 93.8 MPa. Following preliminary studies, De Oliveira *et al.* (2010) presented experimental results of 32 circular STCC columns with various lengths and steel thicknesses, and concrete grades of C30, C60, C80 and C100, then a comparison between test results and predictions from some previous analytical models was conducted to assess the passive confinement and the possibility of these analytical models in calculating the axial load capacity. At the same time, Yu *et al.* (2010) carried out a numerical study on STCC stub columns to investigate the confinement

Table 1 Sequence to calculate the stress-strain curve of confined concrete in four selected models
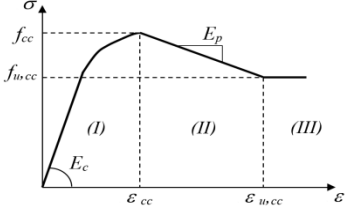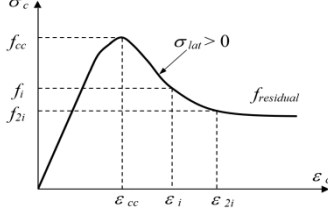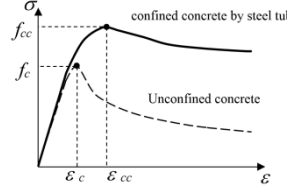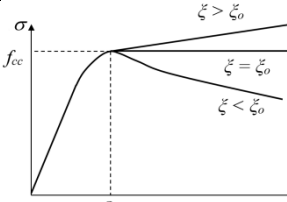
Model	Expressions	Explanations

Hatzigeorgiou (2008)

Region (I):

$$\sigma = A\varepsilon + B\varepsilon^2 + C\varepsilon^3; A = E_c; B = \frac{3f_{cc} - 2E_c\varepsilon_{cc}}{\varepsilon_{cc}^2}; C = \frac{E_c\varepsilon_{cc} - 2f_{cc}}{\varepsilon_{cc}^3}$$

Region (II): $\sigma_{u,cc} = 0.06f_c^{-0.7} + 0.003f_{rp}$

Region (III): $f_{u,cc} = f_{cc} + E_p(\sigma_{u,cc} - \varepsilon_{cc})$

$$\sigma_h = f_y \cdot \exp\left[\ln\left(\frac{D}{t}\right) + \ln(f_y) - 11\right] \text{ in MPa}$$

$$E_p = -1500\left[1 - \left(1 + \exp\left(\frac{D.f_c}{t.f_y} - 6\right)\right)^{-1}\right]$$

$$f_{rp} = \frac{2 \cdot t}{D - 2 \cdot t} \cdot \sigma_h \quad \text{and} \quad f_{yc} = 0.5 \cdot \left(\sigma_h - \sqrt{4 \cdot f_y^2 - 3 \cdot \sigma_h^2}\right)$$

$$\varepsilon_{cc} = 0.0022\frac{f_{cc}}{f_c}; \quad f_{cc} = f_c + 4.3 \cdot f_{rp} \text{ and } N_u = A_c \cdot f_{cc} + A_s \cdot f_{yc}$$

Explanations:

σ_h : Hoop stress of the steel tube

f_{rp} : Mean confining stress

f_{yc} : Compressive yield stress of steel tube

$\sigma_{u,cc}$: linearly decrescent stress

E_p : Inelastic modulus describing the slope of softening branch

$f_{u,cc}$: constant stress in region (III)

Johansson (2002)

$$Y = \frac{AX + BX^2}{1 + CX + DX^2}; Y = \frac{\sigma_c}{f_{cc}}; X = \frac{\varepsilon_c}{\varepsilon_{cc}}; \forall X \geq 0, 0 \leq Y \leq 1$$

When $\varepsilon_c \leq \varepsilon_{cc}$: $A = \frac{E_c\varepsilon_{cc}}{f_{cc}}; B = \frac{(A-1)^2}{\left(1 - 0.45\frac{f_c}{f_{cc}}\right)} - 1; C = A - 2; D = B + 1$

When $\varepsilon_c > \varepsilon_{cc}$: $A = \left[\frac{\varepsilon_{2i} - \varepsilon_i}{\varepsilon_{cc}}\right]\left[\frac{\varepsilon_{2i}\left(\frac{f_i}{\varepsilon_i}\right)}{f_{cc} - f_i} - \frac{4\varepsilon_i\left(\frac{f_{2i}}{\varepsilon_{2i}}\right)}{f_{cc} - f_{2i}}\right]$

$$B = (\varepsilon_i - \varepsilon_{2i})\left[\frac{\left(\frac{f_i}{\varepsilon_i}\right)}{f_{cc} - f_i} - \frac{4\frac{f_{2i}}{\varepsilon_{2i}}}{f_{cc} - f_{2i}}\right]; \quad v_a = 0.3, v_c = 0.2, \varepsilon_v = 0.002$$

$$\varepsilon_{ahr} = \frac{\varepsilon_v(v_a - v_c)}{\left[1 + \frac{2 \cdot t \cdot E_a}{(D - 2 \cdot t) \cdot E_c}\right]} \quad \text{and} \quad \varepsilon_{ah} = -v_a \cdot \varepsilon_v + \varepsilon_{ahr}$$

$$\sigma_{ah} = \frac{E_a}{1 - v_a^2} \cdot (\varepsilon_{ah} + v_a \cdot \varepsilon_{al}); \sigma_{al} = \frac{E_a}{1 - v_a^2} \cdot (\varepsilon_v + v_a \cdot \varepsilon_{ah})$$

$$\sigma_{lat} = \sigma_{ah} \cdot \frac{2 \cdot t}{D - 2 \cdot t} \quad \text{and} \quad k = 1.25 \cdot \left(1 + 0.062 \cdot \frac{\sigma_{lat}}{f_{ct}}\right) \cdot f_c^{-0.21}$$

$$\varepsilon_{cc} = \varepsilon_c \cdot \left(1 + (17 - 0.06f_c)\left(\frac{\sigma_{lat}}{f_c}\right)\right)$$

$$f_{cc} = f_c \cdot \left(\frac{\sigma_{lat}}{f_{ct}} + 1\right)^k \quad \text{and} \quad N_u = A_c \cdot f_{cc} + A_s \cdot \sigma_{al}$$

Explanations:

v_a, v_c : Initial considered values of Poisson's ratio of steel and concrete, respectively.

ε_v : Initial considered values of unconfined concrete

ε_{ahr} : Restrained steel strain

ε_{ah} : Final lateral strain of steel

σ_{ah} : Steel's lateral stress

σ_{al} : Steel's longitudinal stress

σ_{lat} : Compressive confining pressure

k : Parameter that reflects the effectiveness of confinement

f_{ct} : Tensile strength of concrete

E_a : Elastic modulus of steel tube

ε_i, f_i : Strain and Stress for the inflexion point on the descending branch of confined concrete

$\varepsilon_{2i} = 2\varepsilon_i - \varepsilon_c$

Table 1 Continued

Sakino *et al.* (2004)	$$Y=\frac{VX+(W-1)X^2}{1+(V-2)X+WX^2};X=\frac{\varepsilon}{\varepsilon_{cc}};Y=\frac{\sigma}{f_{cc}};V=\frac{E_c\varepsilon_{cc}}{f_{cc}}$$ $$W=1.5-17.1\times10^{-3}f_c+2.39\sqrt{\sigma_{re}}$$ $$E_c=\left(6.9+3.32\sqrt{f_c}\right)\times10^3;\varepsilon_c=0.94(f_c)^{1/4}\times10^{-3}$$ $$\frac{\varepsilon_{cc}}{\varepsilon_c}=\begin{cases}1+4.7(K-1)\forall K\le1.5\\3.4+20(K-1)\forall K>1.5\end{cases};\ K=\frac{f_{cc}}{f_c}$$ $$\sigma_{re}=\frac{k}{k_e}\sigma_r;\sigma_r=\frac{-2\cdot t}{D-2\cdot t}\cdot\sigma_{s\theta};k=4.1\text{ and }k_e=23$$ $$\sigma_{s\theta}=\alpha_u\cdot\sigma_{sy}\text{ and }\sigma_{sz}=\beta_{uc}\cdot\sigma_{sy};\alpha_u=-0.19;\beta_{uc}=0.89$$ $$f_{cc}=\gamma_u\cdot f_c+4.1\cdot\sigma_r;\gamma_u=1.67\cdot D_c^{-0.112}$$ $$N_u=A_c\cdot f_{cc}+A_s\cdot\sigma_{sz}$$	γ_u : Strength reduction factor for concrete σ_r : Lateral confining pressure $\sigma_{s\theta}$: Hoop stress of steel tube in yield condition σ_{sy} : Tensile yield stress of steel σ_{sz} : Axial stress of steel tube in yield Condition σ_{re} : Effective lateral pressure provided by steel tube K: Strength enhancement of confined concrete
Han *et al.* (2005)	Ascending branch: $y=2x-x^2\ (x\le1)$ Descending branch: $y=\begin{cases}1+q\left(x^{0.1\xi}-1\right)\forall\xi\ge1.12\\\dfrac{x}{\beta(x-1)^2+x}\forall\xi<1.12\end{cases}(x>1)$ $$x=\frac{\varepsilon}{\varepsilon_{cc}};y=\frac{\sigma}{\sigma_{cc}};f_{cc}=\left[1+\left(-0.54\xi^2+0.4\xi\right)\left(\frac{24}{f_c}\right)^{0.45}\right]f_c$$ $$\varepsilon_{cc}=\varepsilon_c+\left[1400+800\left(\frac{f_c}{24}-1\right)\right]\xi^{0.2};q=\frac{\xi^{0.745}}{2+\xi}$$ $$\beta=\left(2.36\times10^{-5}\right)^{\left[0.25+(\xi-0.5)^7\right]}f_c\times3.51\times10^{-4}$$	ξ : Confinement factor

mechanism through observations of stress-strain curves in both concrete core and steel tube. Ding *et al.* (2017) have recently developed a combined numerical and theoretical study on the composite action between the concrete core and the steel tube in circular STCC stub columns under axial loading, which was based on the elasto-plastic model. These authors have reached a conclusion that the appropriate friction coefficient between the concrete core and the steel tube ranges between 0.4 and 0.6. Likewise, An and Fehling (2016, 2017a, 2017b) have recently conducted a numerical study and subsequent analysis of the axial stress-strain curves of UHPC confined by circular steel tube. In fact, all existing confining stress-strain models as mentioned above were build up for NSC or HSC and their adoption for UHPC is still questionable. For this reason, it is necessary to develop a new confining stress-strain model for circular STCC columns using UHPC infilled.

To address the aforementioned research gap, as a part of a combined experimental and analytical research which aimed at investigating the strength and ductility of circular STCC stub columns using UHPC, this study attempts to recalibrate the confining stress-strain models proposed by Johansson (2002), Sakino *et al.* (2004), Han *et al.* (2005), Hatzigeorgiou (2008) based on the test results of circular STCC columns using UHPC in the study conducted by Schneider (2006). To achieve this goal, some modifications to the peak confined UHPC strength and its corresponding strain in these models were conducted. In addition, a new confining stress-strain model for confined UHPC in circular STCC stub columns were also proposed and compared with the four models and previous experimental results as well.

2. Summary of axial stress-strain models for concrete confined by steel tube

The stress-strain model for concrete confined by steel tube essentially consists of equations defining the ascending

Table 2 Detail of tested specimens and test results in Schneider (2006)

| No	ID	D (mm)	t (mm)	L (mm)	f_c (MPa)	ε_c	f_y (MPa)	ξ	ε_{cc}	N_r (kN)	N_u (kN)
1	NB2.5	164.2	2.5	652	166.8	0.00356	377	0.144	0.0038	2167	3501
2	NB3.0	189.0	3.0	756	166.8	0.00373	398	0.159	0.00422	3000	4837
3	NB4.0	168.6	3.9	648	174.2	0.00419	363	0.207	0.00557	2400	4216
4	NB4.8	169.0	4.8	645	176.7	0.00415	399	0.280	0.00567	3000	4330
5	NB5.0	168.7	5.2	645	170.5	0.00389	405	0.322	0.00599	3350	4751
6	NB5.6	168.8	5.7	650	173.4	0.00402	452	0.391	0.00684	3455	4930
7	NB8.0	168.1	8.1	645	174.9	0.00365	409	0.525	0.00684	4150	5254
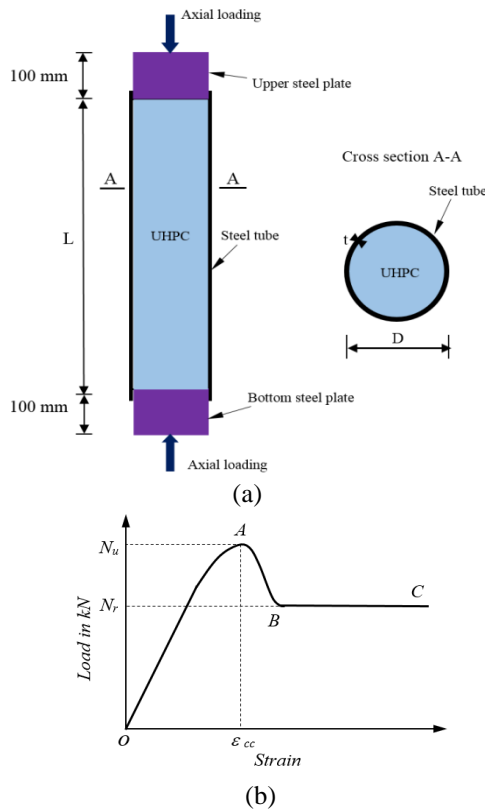
Fig. 1 Schematic view of circular STCC stub columns (a) and general axial load versus strain curve in tests of Schneider (2006)

branch up to the peak stress and the descending branch after the peak stress. The important key of these equations is the confining pressure provided by the steel tube, which is taken into account in the calculation of confined peak stress and strain. Most of existing stress-strain models for confined concrete are based on the assumption that the confining pressure induced by the steel tube is constant during the loading process. However, Johansson proposed a stress-strain model which accounts for the varying confining pressure by using equations of the lateral dilation of concrete. In this study, four confining stress-strain models proposed by Johansson (2002), Sakino *et al.* (2004), Han *et al.* (2005), Hatzigeorgiou (2008) were selected and adopted for estimating the confined peak stress and strain, and stress-strain curves of UHPC confined by steel tube after recalibrating based on test results of circular STCC stub columns in Schneider (2006). These models are able to predict the stress-strain curve of concrete confined by steel

tube stub column encompassing a wide range of values of the significant variables such as concrete compressive strength (f_c), steel yield strength (f_y) and diameter-to-thickness ratio (D/t) with relatively good accuracy as compared to other existing models. The sequence of procedures to predict the stress-strain curve of confined concrete, confined peak stress (f_{cc}) and strain (ε_{cc}), and ultimate load (N_u) in each model is shown in Table 1.

3. Recalibration of confined peak stress and strain in four models

Except for the test database published by Schneider (2006), Xiong (2012), to the best knowledge of the authors, up to date, no available experimental work has been reported on circular STCC stub columns using UHPC with the compressive strength of concrete cylinder higher than 150 MPa under axial loading. Consequently, in this study, a total of seven circular STCC stub columns tested by Schneider (2006) were chosen for the assessment and the recalibration of confined peak stresses and strains calculated by four models in Table 1. The detail of dimensions, material properties and test results of seven specimens in Schneider (2006) were illustrated in Table 2. It should be noted that, in Schneider (2006), coarse aggregate (using Basalt split) UHPC without fibers and having self compacting characteristics was used. It is also important to find that the strain of UHPC core in Schneider's tests was directly measured over a length of 300 mm using three Linear Varying Displacement Transducers (LVDTs) which monitored the displacement of steel bars positioned in the concrete core through an arrangement of drillings in the steel tube (Tue *et al.* 2004a)

For the convenience of comparison and analysis in this study, the confinement factor (ξ), which has been commonly introduced to reflect the combined effects of steel tube and concrete core on the column strength, was used and defined as the following equation

$$\xi = \frac{A_s . f_y}{A_c . f_c} \tag{1}$$

in which A_s is the cross-sectional area of steel tube, A_c is the cross-sectional area of concrete, f_y is the yield strength of steel tube, and f_c is the compressive strength of concrete cylinder.

The confined peak stress f_{cc} can be defined through the ratio of ultimate load (N_u) to concrete cross-sectional area,
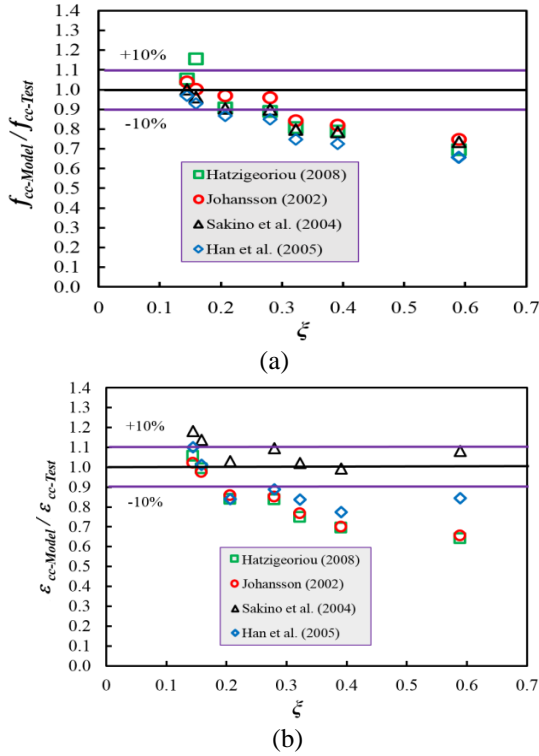
Fig. 2 The ratio $f_{cc\text{-}Model} / f_{cc\text{-}Test}$ versus the confinement factor ξ (a) and the ratio $\varepsilon_{cc\text{-}Model} / \varepsilon_{cc\text{-}Test}$ versus the confinement factor ξ (b)

which is given by the following equation

$$f_{cc} = \frac{N_u}{A_c} \qquad (2)$$

N_r is defined as the second peak load where the axial load-strain curve is supposed to be approximately horizontal (see Fig. 1(b)).

3.1 Comparison of confined peak stress and strain in four models with previous test results

The confined peak stress and strain predicted by four models in Table 1 and taken from test results in Table 2 were denoted as $f_{cc\text{-}Model}$, $\varepsilon_{cc\text{-}Model}$ and $f_{cc\text{-}Test}$, $\varepsilon_{cc\text{-}Test}$, respectively. In order to perform the comparisons between the test results and the models, the ratios $f_{cc\text{-}Model}/f_{cc\text{-}Test}$ versus the confinement factor ξ and the ratios $\varepsilon_{cc\text{-}Model}/\varepsilon_{cc\text{-}Test}$ versus the confinement factor ξ were plotted in Fig. 1(a) and Fig. 1(b), respectively. It is evident from Fig. 2(a)-(b) that the prediction accuracy of four models is generally decreased with the increase in the confinement factor ξ. In particular, all models showed very large underestimations of the confined peak stress f_{cc} and the confined peak strain ε_{cc} with the values of ξ higher than 0.3. Among four models, the model proposed by Johansson (2002) gave the best prediction of the confined peak stress f_{cc}, while the model of Sakino *et al.* (2004) exhibited the closest prediction of the confined peak strain ε_{cc} as compared to the test results. From these observations, it is necessary to make some modifications to these models in order to obtain closer
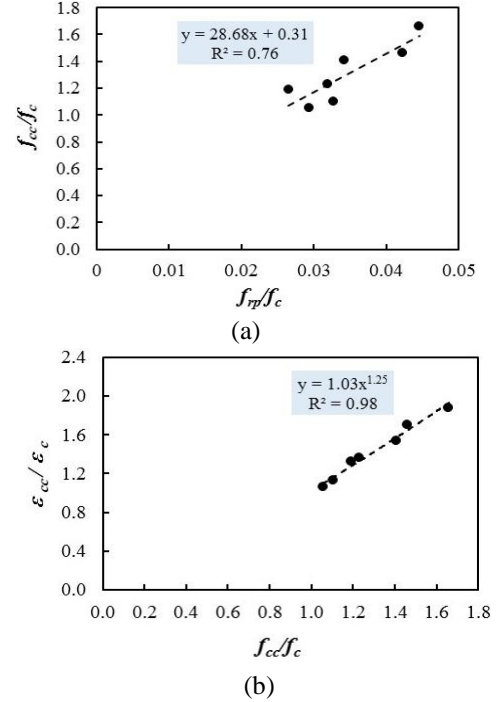

Fig. 3 The relationships between the ratio f_{cc}/f_c and the ratio f_{rp}/f_c (a), the ratio $\varepsilon_{cc}/\varepsilon_c$ and the ratio f_{cc}/f_c (b) for the model of Hatzigeoriou (2008)

predictions of f_{cc} and ε_{cc} as compared to the test results.

The modulus of elasticity E_c and the strain ε_{cc} at the peak stress f_c of unconfined UHPC in this study can be calculated using the following equations proposed by Schneider (2006)

$$E_c = 10200 \cdot f_c^{1/3} \qquad (3)$$

$$\varepsilon_c = 0.00083 \cdot f_c^{0.276} \qquad (4)$$

The lateral confining stress was computed using the experimental database in Table 2 and the equations from the models in Table 1. The ratios f_{cc}/f_c and $\varepsilon_{cc}/\varepsilon_c$ was calculated using actual test results in Table 1. Afterwards, the relationships between the ratios f_{cc}/f_c and f_{rp}/f_c (or σ_{lat}/f_c, σ_r/f_c), the ratios $\varepsilon_{cc}/\varepsilon_c$ and the ratios f_{cc}/f_c, the ratios $\varepsilon_{cc}/\varepsilon_c$ and the ratios f_{rp}/f_c were established in order to consider the regression analysis. Based on these relationships with relatively high regression coefficients (R^2), the equations for predicting f_{cc} and ε_{cc} were modified in each model.

3.2 Modification of equations in the model of Hatzigeorgiou (2008)

Based on the relationships between the ratios f_{cc}/f_c and f_{rp}/f_c, the ratios $\varepsilon_{cc}/\varepsilon_c$ and the ratios f_{cc}/f_c plotted in Fig. 3, the equations for predicting the confined peak stress f_{cc} and strain ε_{cc} can be modified as follows

$$\frac{f_{cc}}{f_c} = 0.31 + 28.68 \frac{f_{rp}}{f_c} \qquad (5)$$

$$\frac{\varepsilon_{cc}}{\varepsilon_c} = 1.03 \left(\frac{f_{cc}}{f_c} \right)^{1.25} \qquad (6)$$
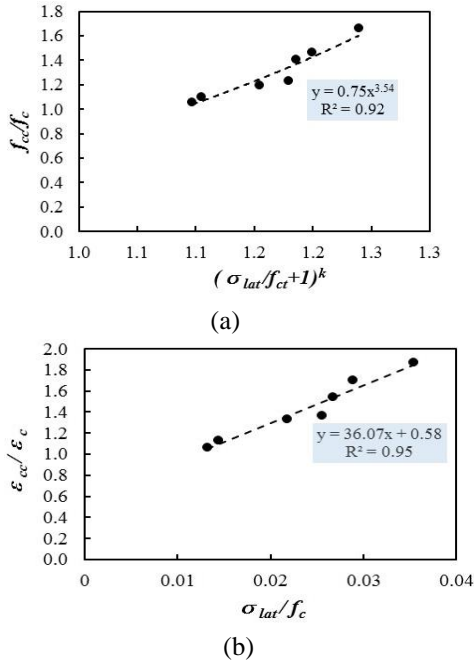
(a)

(b)

Fig. 4 The relationships between the ratio f_{cc}/f_c and the ratio f_{rp}/f_c (a), the ratio $\varepsilon_{cc}/\varepsilon_c$ and the ratio f_c/f_c (b) for the model of Johansson (2002)
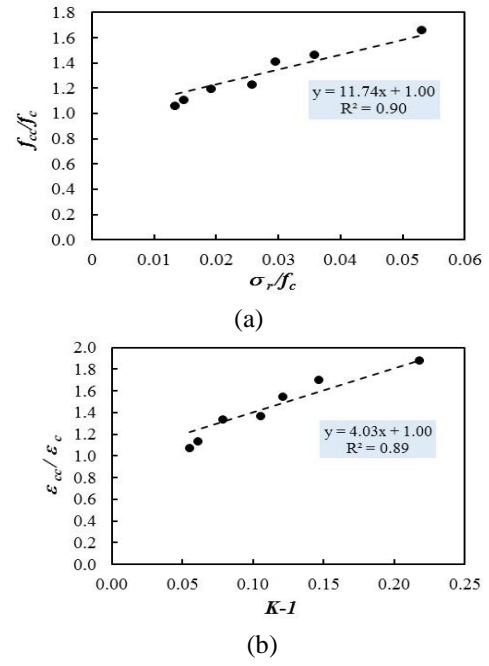

(a)

(b)

Fig. 5 The relationships between the ratio f_{cc}/f_c and the ratio f_{rp}/f_c (a), the ratio $\varepsilon_{cc}/\varepsilon_c$ and the ratio f_c/f_c (b) for the model of Sakino *et al.* (2004)

3.3 Modification of equations in the model of Johansson (2002)

As shown in Table 1, the tensile strength of concrete f_{ct} is used in the equation for predicting the confined peak stress in the model of Johansson (2002). This approach is quite different from the other models which usually do not consider the effect of f_{ct} on the confined strength. For UHPC, the tensile strength of concrete f_{ct} can be estimated using the formula proposed by Fehling *et al.* (2014) as given below

$$f_{ct} = 0.3 \cdot \left(f_c\right)^{2/3} \tag{7}$$

Beside the relationship between the ratios $\varepsilon_{cc}/\varepsilon_c$ and the ratios f_{cc}/f_c illustrated in Fig. 4(b), the relationship between the ratios f_{cc}/f_c and the values $(f_{rp}/f_{ct}+1)^k$ was also established in Fig. 4(a). Due to good correlation obtained from these relationships, the modified equations for predicting the confined peak stress f_{cc} and strain ε_{cc} can be given as follows

$$\frac{f_{cc}}{f_c} = 0.75\left(\frac{\sigma_{lat}}{f_{ct}} + 1\right)^{3.54k} \tag{8}$$

$$\frac{\varepsilon_{cc}}{\varepsilon_c} = 0.58 + 36.07\frac{\sigma_{lat}}{f_c} \tag{9}$$

3.4 Modification of equations in the model of Sakino et al. (2004)

As shown in Table 1, in the model of Sakino *et al.* (2004), the ratio $\varepsilon_{cc}/\varepsilon_c$ was expressed in terms of the strength enhancement factor K which was defined as the

ratio f_{cc}/f_c. Therefore, following the original equation for calculating the ratio $\varepsilon_{cc}/\varepsilon_c$ in this approach, the relationship between the ratios $\varepsilon_{cc}/\varepsilon_c$ and the values of K-1 was built up in Fig. 5b. Additionally, the relationship between the ratios f_{cc}/f_c and the ratios f_{rp}/f_c was plotted in Fig. 5a. It can be seen in Fig. 5(a)-(b), there are also strong positive correlations in these relationships, thus the formulae for predicting the ratio f_{cc}/f_c and the ratio $\varepsilon_{cc}/\varepsilon_c$ are recalibrated as

$$\frac{f_{cc}}{f_c} = 1 + 11.74\frac{\sigma_r}{f_c} \tag{10}$$

$$\frac{\varepsilon_{cc}}{\varepsilon_c} = 1 + 4.03(K-1) \tag{11}$$

3.5 Modification of equations in the model of Han et al. (2005)

In the model of Han *et al.* (2005), the confinement factor ξ was adopted as a main parameter in the formulae for predicting the ratio f_{cc}/f_c and $\varepsilon_{cc}/\varepsilon_c$. As a consequence, the relationships between the ratio f_{cc}/f_c and the confinement factor ξ, the value $(\varepsilon_{cc}-\varepsilon_c)$ and the confinement factor ξ were established through the test database in Table 2 and then illustrated in Fig. 6(a)-(b), respectively. Accordingly, the equations for predicting the peak confined stress f_{cc} and strain ε_{cc} can be rewritten as

$$f_{cc} = \left(1 + 0.8\xi + 0.63\xi^2\right)f_c \tag{12}$$

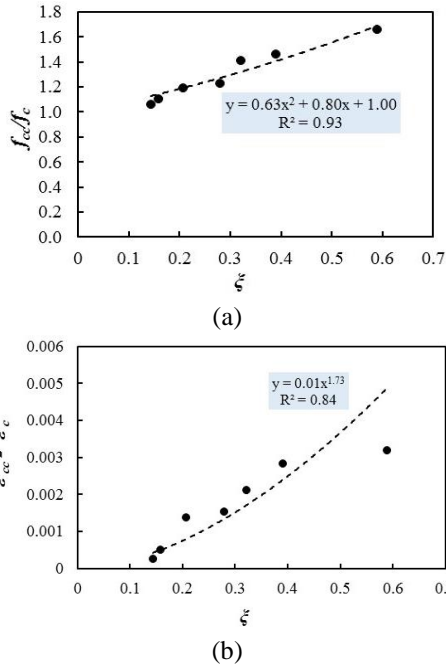$$\varepsilon_{cc} = \varepsilon_c + 0.01\xi^{1.73} \tag{13}$$

(a)

(b)

Fig. 6 The relationships between the ratio f_{cc}/f_c and the confinement factor ξ (a), The value $(\varepsilon_{cc} - \varepsilon_c)$ versus the confinement factor ξ (b) for the model of Han *et al.* (2005)
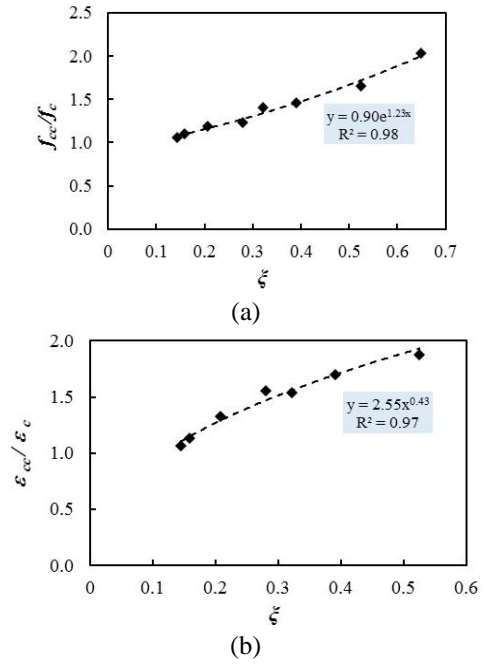

(a)

(b)

Fig. 8 The relationships between the ratio f_{cc}/f_c and the confinement factor ξ (a), the ratio $\varepsilon_{cc}/\varepsilon_c$ versus the confinement factor ξ (b) obtained from Schneider (2006)
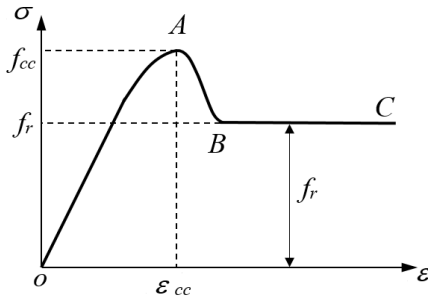

Fig. 7 Stress-strain model proposed for confined UHPC

3.6 Proposed model for axial stress-strain curve of confined UHPC by steel tube

For the purpose of modelling the confinement effect in circular STCC stub columns, a proposed axial stress-strain model of confined UHPC incorporating the confinement effect has been derived based on the test results of Schneider (2006) as given in Table 1 and the models proposed by Binici (2005), Tao *et al.* (2013) and Samani and Attard (2012). From the observations of axial load-strain of circular STCC stub columns with various steel tube thicknesses in Schneider (2006), a general axial stress-strain model for confined UHPC can be divided in three regions, the ascending (OA), the descending (AB) and the constant stress branch (BC), as demonstrated in Fig. 7.

The ascending stress-strain (σ-ε) curve (OA) is represented using the equations suggested by Samani and Attard (2012) for confined concrete as follows

$$Y = \frac{A \cdot X + B \cdot X^2}{1 + (A-2) \cdot X + (B+1) \cdot X^2} \quad \text{when} \quad 0 \le \varepsilon \le \varepsilon_{cc} \quad (14)$$

where

$$Y = \frac{\sigma}{f_{cc}} \quad \forall \ 0 \le Y \le 1 \tag{15}$$

$$X = \frac{\varepsilon}{\varepsilon_{cc}} \quad \forall \ X \ge 0 \tag{16}$$

$$A = \frac{E_c \cdot \varepsilon_{cc}}{f_c} \tag{17}$$

$$B = \frac{(A-1)^2}{0.55} - 1 \tag{18}$$

It should be noted that the axial stress-strain model for confined concrete proposed by Samani and Attard (2012) is applicable to a wide range of concrete compressive strength from 20 to 130 MPa.

The authors found that based on the regression analysis obtained from the test database of Schneider (2006) as shown in Fig. 8(a)-(b), the peak confined stress f_{cc} and corresponding strain ε_{cc} of UHPC can be expressed as functions of confinement factor ξ

$$\frac{f_{cc}}{f_c} = 0.9 \cdot e^{1.23 \cdot \xi} \tag{19}$$

$$\frac{\varepsilon_{cc}}{\varepsilon_c} = 2.55 \cdot \xi^{0.43} \tag{20}$$

where the strain ε_c at peak stress under uniaxial compression and the elastic modulus E_c are calculated according to the Eqs. (3)-(4).

For the descending branch (AB) and the constant stress branch (BC), an exponential function proposed by Binici
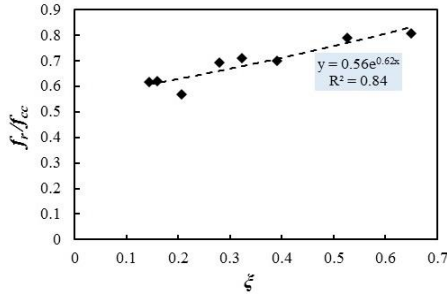
Fig. 9 The relation between f_r/f_{cc} and ξ obtained from Schneider (2006)

(2005) is used and given by

$$\sigma = f_r + (f_{cc} - f_r)\exp\left[-\left(\frac{\varepsilon - \varepsilon_{cc}}{\alpha}\right)^\beta\right] \quad \text{when} \quad \varepsilon > \varepsilon_{cc} \quad (21)$$

in which f_r is the residual stress as shown in Fig. 7. It is mentioned that f_r can be denoted as the residual stress at the second peak load N_r. As a result, f_r is calculated using the ratio of the second peak load (N_r) to concrete cross-sectional area (A_c)
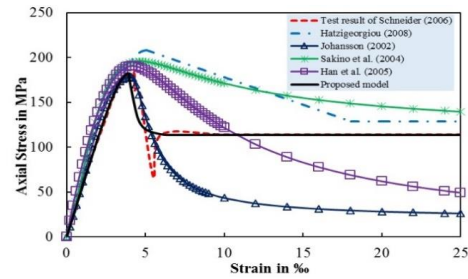
$$f_r = \frac{N_r}{A_c} \quad (22)$$

The expression for f_r can be proposed by the result of regression analysis of the ratios f_r/f_{cc} and the confinement factor ξ in Fig. 9 as follows

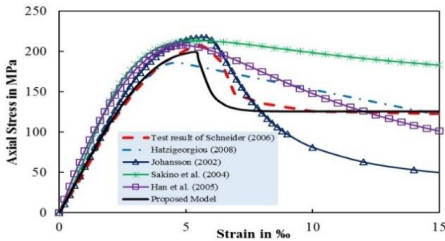$$\frac{f_r}{f_{cc}} = 0.56 \cdot e^{0.62 \cdot \xi} \quad (23)$$

In Eq. (21), α and β are parameters determining the shape of the softening branch (AB and BC). The value of α is expressed following Tao *et al.* (2013)
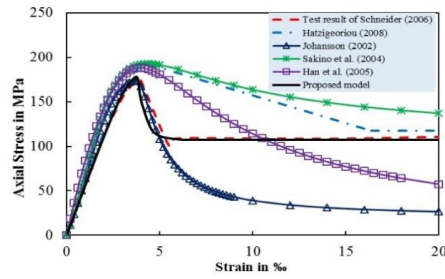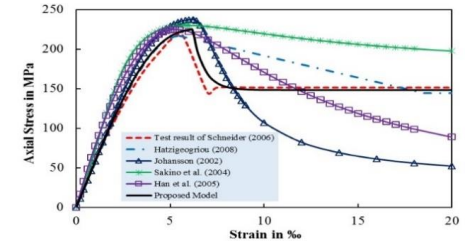

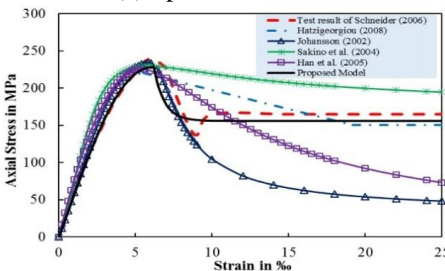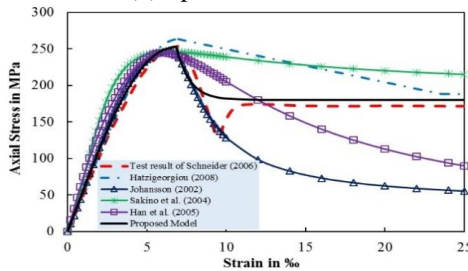
(a) Specimen NB2.5

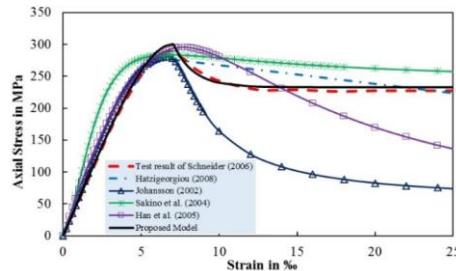(b) Specimen NB3.0

(c) Specimen NB4.0

(d) Specimen NB4.8

(e) Specimen NB5.0

(f) Specimen NB5.6

(g) Specimen NB8.0

Fig. 10 Comparison of modified models and proposed model with test results in Schneider (2006)

Table 3 Dimensions and material properties of specimens for parametric study

Specimens	Dimensions					Material properties		ξ
	D (mm)	t (mm)	D/t	L (mm)	L/D	f_c (MPa)	f_y (MPa)	
Group 1 – To examine the effects of concrete strength f_c								
C1	150	4.0	37.5	450	3.0	**150**	350	0.270
C2	150	4.0	37.5	450	3.0	**160**	350	0.253
C3	150	4.0	37.5	450	3.0	**170**	350	0.239
C4	150	4.0	37.5	450	3.0	**180**	350	0.225
C5	150	4.0	37.5	450	3.0	**190**	350	0.213
C6	150	4.0	37.4	450	3.0.	**200**	350	0.203
C7	150	4.0	37.5	450	3.0	**210**	350	0.193
C8	150	4.0	37.5	450	3.0	**220**	350	0.184
C9	150	4.0	37.5	450	3.0	**230**	350	0.176
Group 2 – To examine the effects of steel yield strength f_y								
C10	150	5.0	30.0	450	3.0	190	**230**	0.179
C11	150	5.0	30.0	450	3.0	190	**290**	0.226
C12	150	5.0	30.0	450	3.0	190	**350**	0.273
C13	150	5.0	30.0	450	3.0	190	**390**	0.304
C14	150	5.0	30.0	450	3.0	190	**460**	0.358
Group 3 – To examine the effects of the ratio D/t								
C15	150	3.0	**50.00**	450	3.0	30	350	0.165
C16	150	4.0	**37.50**	450	3.0	30	350	0.225
C17	150	5.0	**30.00**	450	3.0	30	350	0.288
C18	150	6.0	**25.00**	450	3.0	30	350	0.353
C19	150	7.0	**21.43**	450	3.0	90	350	0.421
C20	150	8.0	**18.75**	450	3.0	90	350	0.492
C21	150	9.0	**16.67**	450	3.0	90	350	0.566
C22	150	10.0	**15.00**	450	3.0	180	350	0.644

$$\alpha = 0.04 - \frac{0.036}{1 + e^{6.08\xi - 3.49}} \qquad (24)$$

To ensure the predicted softening branch of axial stress-strain curves match with measured values of test results in Schneider (2006) closely, different trial values of β were adopted. The authors found that when β was equal to 15, the predicted curves were acceptable compared with the experimental curves. Thus, β is taken as 15.

It should be mentioned that the validity of the proposed model is: $f_c \geq 150$ MPa and $235 \leq f_y$ (MPa) ≤ 460, and $0.15 \leq \xi \leq 0.6$.

4. Comparison of modified models and proposed model with previous test results

The modified models and proposed model were used to predict the axial stress-strain curves for confined UHPC of specimens tested by Schneider (2006). Fig. 10 (a)-(g) compare the predicted axial stress-strain curves with the test results of Schneider (2006). It can be seen from Fig. 10 (a)-(g) that although the confined peak stress and corresponding strain of tested specimens can be accurately estimated using the modified models, these models are not satisfactory in predicting the complete axial stress-strain curves. There is a

large difference in predicting the descending branch between the modified models and test results. However, the model of Johansson (2002) gives a very close ascending branch compared to that obtained from the test results. In addition, the model of Johansson (2002) also performs an abrupt drop of load after the first peak load, but the predicted constant stress branch is lower than that in the test results. Among all models, the model of Johansson (2002) is supposed to be potentially applicable to predict the ascending branch.

As evident from the comparisons in Fig. 10, the predicted axial stress-strain curves of the proposed model agree reasonably well with the experimental results. Furthermore, the sudden load drop in the softening branch of stress-strain curves right after the first peak stress and the constant stress branch after the second peak stress are very well described by the proposed model. Therefore, the proposed model can be further adopted to investigate the compressive behavior of circular STCC stub columns using UHPC through axial stress-strain curves of confined UHPC, thereby saving cost and time of experiments.

5. Parametric study using the proposed model

As is well known, the behavior of axially loaded circular STCC stub columns is mainly affected by diameter-to-thickness ratio (D/t), steel yield strength (f_y) and concrete compressive strength (f_c). Once the proposed model was verified, it was utilized to perform a parametric study for circular STCC stub columns with a wide range of D/t, f_y and f_c. Afterwards, the influences of D/t, f_y and f_c on the compressive behavior of circular STCC stub columns were examined. Table 4 shows the characteristics of the specimens including three groups, which were adopted for the parametric study using the proposed model.

The influence of D/t, f_y and f_c on the compressive behavior of circular STCC stub columns using UHPC were shown using not only the complete axial stress-strain curve of confined UHPC but also the strength enhancement expressed by the ratio f_{cc}/f_c and the strain enhancement expressed by the ratio $\varepsilon_{cc}/\varepsilon_c$.

5.1 Effects of concrete compressive strength

The influence of concrete compressive strength on the behavior of circular STCC stub columns in group 1 of Table 3 is illustrated in Fig. 11. Fig. 11(a) shows the predicted axial stress-strain curves of confined UHPC for the concrete compressive strength ranging between 150 MPa and 230 MPa. It can be observed from Fig. 11(a) that there is no change in the general shape of axial stress-strain curves regardless of various compressive strengths. Otherwise, the increase in the compressive strength results in steeper descending branch after the first peak load and slightly reduces the ratio f_r/f_{cc}. The predicted strength enhancement and the predicted ductility enhancement for each case of concrete compressive strength were plotted in Fig. 11(b). As can be seen in Fig. 11(b), the strength enhancement and the ductility enhancement linearly decreases with the increase in the concrete compressive strength. For instance, with the
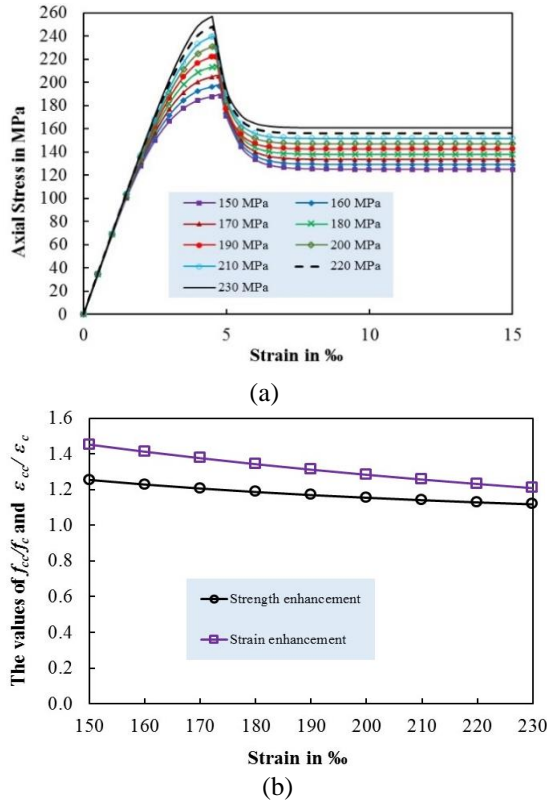
(a)

(b)

Fig. 11 Effect of concrete compressive strength f_c on: the axial stress strain of confined UHPC (a); the strength and strain enhancement (b)

(a)

(b)

Fig. 12 Effect of steel yield strength f_y on: the axial stress strain of confined UHPC (a); the strength and strain enhancement (b)

concrete compressive strength of 150 MPa, 190 MPa and 230 MPa, the peak confined stress (f_{cc}) is increased by 25.5%, 17% and 11.8% as compared to unconfined compressive strength (f_c), respectively, while the peak confined strain (ε_{cc}) is increased by 45.5%, 31.3% and 20.9% as compared to unconfined strain (ε_c), respectively. It is briefly concluded that higher concrete compressive strength leads to less ductility and strength enhancement, and strain enhancement than the lower one.

5.2 Effects of steel yield strength

Fig. 12 depicts the influence of steel yield strength on the behavior of circular STCC stub columns in group 2 of Table. The predicted axial stress-strain curves of confined UHPC for the steel yield strength ranging between 230 MPa and 460 MPa were illustrated in Fig. 12(b). It is pointed out from Fig. 12(a) that increasing the steel yield strength does not change the general shape of axial stress-strain curves. However, the initial axial stiffness of confined UHPC is considerably affected by the steel yield strength. The ratio f_y/f_{cc} is slightly increased with higher steel yield strength. The predicted strength and strain enhancement with various steel yield strengths are plotted in Fig. 12(b). As evident from Fig. 12(b), the strength and strain enhancement of confined UHPC are proportionally increased with an increase the steel yield strength. When increasing the steel yield strength from 230 MPa to 350 MPa and 460 MPa, the strength enhancement is increased by 12.18% and 24.64%,
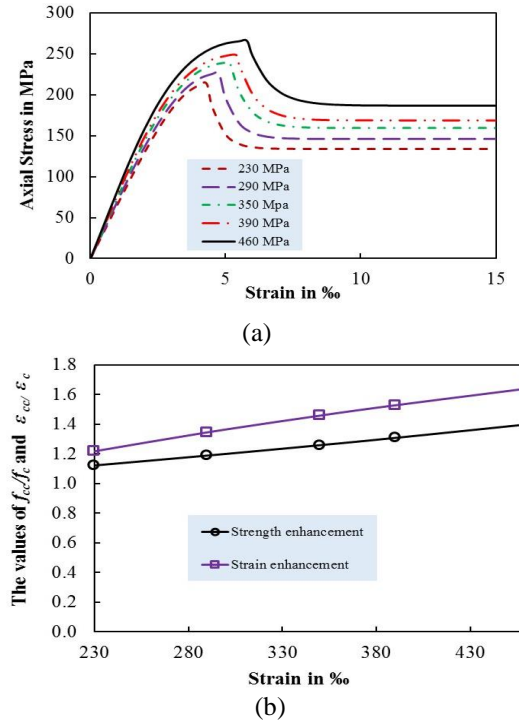
respectively, while the strain enhancement is increased by 19.7% and 34.7%, respectively. From these observations, it can be argued that higher steel yield strength results in better ductility and considerably increases the strength and strain enhancement.

5.3 Effects of the ratio D/t

The effect of the ratio *D/t* on the behavior of circular STCC stub columns in group 3 of Table 3 is presented in Fig. 13. The predicted axial stress-strain curves of confined UHPC for the ratio D/t ranging between 15 and 50 were shown in Fig. 13a. This figure demonstrates that the post-peak behavior of confined UHPC is remarkably affected by the ratio *D/t*. The descending branch after the first peak stress for the columns with lower ratio of *D/t* exhibits more gradual slope than higher ones, thus indicating that lower ratio of *D/t* can lead to an significant improvement in the ductility. In addition, the columns using lower ratios of *D/t* perform larger initial stiffness than that using higher ones. Fig. 13(b) shows the predicted strength and strain enhancement for a wide range of *D/t*. It is revealed from this figure the strength and strain enhancement of confined UHPC are significantly increased with lower ratio of *D/t*. When decreasing the ratio *D/t* from 50 to 21.43 and 15, the strength enhancement is increased by 36.93% and 80.22%, respectively, while the strain enhancement is increased by 49.42% and 79.44%, respectively. Based on these observations, it can be derived that, among the key parameters affecting to the behavior of circular STCC stub columns using UHPC as mentioned above, the ratio *D/t* has a major influence. Not only the ductility but also the
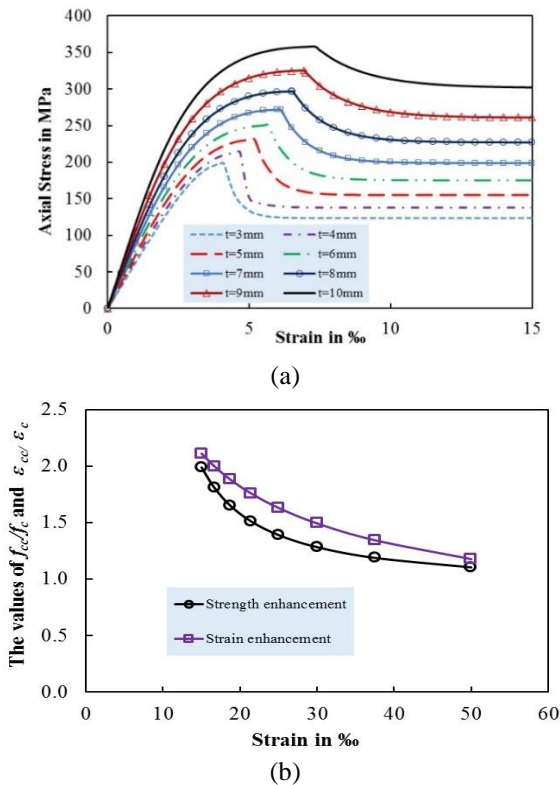
(a)

(b)

Fig. 13 Effect of the ratio *D/t* on: the axial stress strain of confined UHPC (a); the strength and strain enhancement (b)

strength and strain enhancement can be greatly increased when using lower ratio of *D/t*.

6. Conclusions

The objective of this study was an assessment of the axial stress-strain curves from existing models and proposed model for UHPC confined by steel tube stub columns based on the experimental results achieved from Schneider (2006). The following conclusions can be drawn as follows:

- Four axial stress-strain models for confined concrete assumed by Johansson (2002), Sakino *et al.* (2004), Han *et al.* (2005), Hatzigeorgiou (2008) were reviewed. It has been remarked that, among four models, the model of Johansson (2002) exhibited the best prediction of the confined peak stress f_{cc}, while the model of Sakino *et al.* (2004) gave the most accurate prediction of the confined peak strain ε_{cc} in comparison with the test results of Schneider (2006).

- In order to improve the prediction accuracy, based on the regression analysis of test results in Schneider (2006), the equations for calculating the confined peak stress f_{cc} and the confined peak strain ε_{cc} in four models were modified and then a new axial stress-strain model for confined UHPC were proposed. The validity of proposed model is: $f_c \geq 150$ MPa and $235 \leq f_y$ (MPa)≤ 460, and $0.15 \leq \xi \leq 0.6$.

- The suitability of four modified models and proposed model for prediction of axial stress-strain curves of confined UHPC was verified by comparisons with previous test results. It was found that, among four models, only the model of Johansson (2002) is capable of predicting the ascending branch and performing the sudden load drop after the first peak load. In addition, the proposed model gives a very good agreement with the test results, thus indicating that it can be adopted for modeling the compressive behavior of circular STCC stub column using UHPC.

- A parametric study was undertaken employing the proposed model to investigate the effects of diameter-to-thickness ratio (*D/t*), steel yield strength (f_y) and concrete compressive strength (f_c) on the complete axial stress-strain curves, the strength and strain enhancement of circular STCC stub column using UHPC. It was shown that the strength and strain enhancement were found to increase proportionally with increasing the values of f_y and decreasing the values of f_c. Higher compressive strengths result in a lower increase in the strength and strain enhancement as compared to that of lower ones. In addition, the ductility in the post-peak domain is decreased as the values of f_c increase, while it is slightly enhanced with using higher values of f_y. However, the rate of the increase in the strength and its corresponding strain, and the ductility in the post-peak domain for the columns with increasing f_y or f_c is less than that with increasing the ratio *D/t*.

- It was worth noting from this parametric study that, among three key parameters as mentioned, the ratio *D/t* has a major influence on the compressive behavior of confined UHPC. The use of lower ratio of *D/t* (or thicker steel thickness) significantly increases the ductility, strength and strain enhancement of circular STCC stub column.

- Further experimental research is needed to examine the compressive behavior of circular STCC stub column using UHPC with $f_c \geq 150$ MPa and to develop more accurate model of axial stress-strain curve for confined UHPC.

References

Aboutaha, R.S. and Machado, R. (1998), "Seismic resistance of steel confined reinforced concrete (SCRC) columns", *Struct. Des. Tall Build.*, **7**, 251-260.

An L.H., Fehling, E. and Ismail, M. (2016), "Numerical modelling

of circular concrete filled steel tube stub columns", *Proceedings of HiperMat 2016 4ᵗʰ International Symposium on Ultra-High Performance Concrete and High Performance Construction Materials*, Kassel, March.

An, L.H. and Fehling, E. (2016), "Finite element analysis of circular steel tube confined UHPC stub columns", *Rilem proceedings No. 105 of 1ˢᵗ International Conference on UHPC Materials and Structures (UHPC 2016-China)*, Changsha, China, October.

An, L.H. and Fehling, E. (2017a), "Numerical analysis of circular steel tube confined UHPC stub columns", *Comput. Concrete*, **19**(3), 263-273.

An, L.H. and Fehling, E. (2017b), "Analysis of circular steel tube confined UHPC stub columns", *Steel Compos. Struct.*, **23**(6), 669-682.

Binici, B. (2005), "An analytical model for stress-strain behavior of confined concrete", *Eng. Struct.*, **27**(7), 1040-1051.

De Oliveira, W.L.A., De Nardin, S., De Cresce El Debs, A.L.H. and El Debs, M.K. (2010), "Evaluation of passive confinement in CFT columns", *J. Constr. Steel Res.*, **66**(4), 487-495.

Ding, F.X., Tan, L., Liu, X.M. and Wang, L. (2017), "Behavior of circular thin-walled steel tube confined concrete stub columns", *Steel Compos. Struct.*, **23**(2), 229-238.

Empelmann, M., Teutsch, M. and Steven, G. (2008) "Load-bearing behaviour of centrically loaded UHPFRC-columns", *Proceeding of Second International Symposium on Ultra High Performance Concrete*, Kassel, Germany.

Fehling, E., Schmidt, M., Walraven, J., Leutbecher, T. and Fröhlich, S. (2014), *Ultra-High Performance Concrete: Fundamental-Design-Example*, Wilhelm Ernst & Sohn, Verlag für Architektur und technische Wissenschaften GmbH & Co. KG, Rotherstraße 21, 10245 Berlin, Germany.

Graybeal, B.A. (2005), "Characterization of the behavior of ultra-high performance concrete", Ph.D. Dissertation, University of Maryland, USA.

Guler, S. (2014), "Axial behavior of FRP-wrapped circular ultra high performance concrete specimens", *Struct. Eng. Mech.*, **50**(6), 709-722.

Guler, S., Aydogan, M. and Copur, A. (2013), "Axial capacity and ductility of circular UHPC-filled steel tube columns", *Mag. Concrete Res.*, **65**(15), 898-905.

Han, L.H., Li, W. and Bjorhovde, R. (2014), "Development and advanced applications of concrete-filled steel tubular (CFST) structures: members", *J. Constr. Steel Res.*, **100**, 211-228.

Han, L.H., Yao, G.H. and Zhao, X.L. (2005), "Test and calculations for hollow structural steel (HSS) stub columns filled with self-consolidating concrete (SCC)", *J. Constr. Steel Res.*, **61**, 1241-1269

Hatzigeorgiou, G.D. (2008), "Numerical model for the behavior and capacity of circular CFT columns, Part I: Theory", *Eng. Struct.*, **30**(6), 1573-1578.

Hosinieh, M.M., Aoude, H., Cook, W.D. and Mitchell, D. (2015), "Behavior of ultra-high performance fiber reinforced concrete columns under pure axial loading", *Eng. Struct.*, **99**, 388-401.

Huang, F., Yu, X. and Chen, B. (2012), "The structural performance of axially loaded CFST columns under various loading conditions", *Steel Compos. Struct.*, **13**(5), 451-471.

Johansson, M. (2002), "The efficiency of passive confinement in CFT columns", *Steel Compos. Struct.*, **2**(5), 379-396.

Liang, Q.Q. and Fragomeni, S. (2009), "Nonlinear analysis of circular concrete-filled steel tubular short columns under axial loading", *J. Constr. Steel Res.*, **65**(12), 2186-2196.

Liew, J.Y.R. and Xiong, D.X. (2010), "Experimental investigation on tubular columns infilled with ultra-high strength concrete", Tubular Structures XIII, The University of Hong Kong, 637-645.

Liew, J.Y.R. and Xiong, D.X. (2012), "Ultra-high strength concrete filled composite columns for multi-storey building construction", *Adv. Struct. Eng.*, **15**(9), 1487-1503.

Liew, J.Y.R. and Xiong, M.X. (2015), *Design Guide For Concrete Filled Tubular Members With High Strength Materials to Eurocode 4*, Research Publishing, Blk 12 Lorong Bakar Batu, 349568 Singapore.

Liew, J.Y.R., Xiong, M.X. and Xiong, D.X. (2014), "Design of high strength concrete filled tubular columns for tall buildings", *Int. J. High-Rise Build.*, **3**(3), 215-221.

Liew, J.Y.R., Xiong, M.X. and Xiong, D.X. (2016), "Design of concrete filled tubular beam-columns with high strength steel and concrete", *Struct.*, **8**, 215-221.

Liu, J., Zhang, S., Zhang, X. and Guo, L. (2009), "Behavior and strength of circular tube confined reinforced-concrete (CTRC) columns", *J. Constr. Steel Res.*, **65**, 1447-1458.

Liu, S.H., Li, L.H. and Feng, J.W. (2012), "Study on mechanical properties of reactive powder concrete", *J. Civil Eng. Constr.*, **1**(1), 6-11.

Morino, S., Uchikoshi, M. and Yamaguchi, I. (2001), "Concrete-filled steel tube column system-its advantages", *Steel Struct.*, **1**, 33-44.

O'Shea, M.D. and Bridge, R.Q (2000), "Design of circular thin-walled concrete filled steel tubes", *J. Struct. Eng.*, ASCE, **126**(11), 1295-1303.

Sakino, K., Nakahara, H. Morino, S. and Nishiyama, I. (2004), "Behavior of centrally loaded concrete-filled steel-tube short columns", *J. Struct. Eng.*, ASCE, **130**(2), 180-188.

Samani, A.K. and Altard, M.M. (2012), "A stress-strain model for uniaxial and confined concrete under compression", *Eng Struct.*, **41**, 335-349.

Schneider, H. (2006), "Zum tragverhalten kurzer, umschnürter, kreisförmiger, druckglieder aus ungefasertem UHFB", Ph.D. Dissertation, University of Leipzig, Leipzig, Germany. (in German)

Shin, H.O., Soon, Y.S., Cook, W.D. and Michell, D. (2015), "Effect of confinement on the axial load response of Ultrahigh-strength concrete columns", *J. Struct. Eng.*, ASCE, **141**(6), 04014151.

Sun, Y. (2008), "Proposal and application of stress-strain model for concrete confined by steel tubes", *Proceeding of the 14ᵗʰ World Conference on Earthquake Engineering*, October, Beijing, China.

Susantha, K.A.S., Ge, H. and Usami, T. (2001), "Uniaxial stress-strain relationship of concrete confined by various shaped steel tubes", *Eng. Struct.*, **23**(10), 1331-1347.

Tang, J., Hino, S., Kuroda, I. and Ohta, T. (1996), "Modeling of stress-strain relationships for steel and concrete in concrete filled circular steel tubular columns", *Steel Constr. Eng., JSSC*, **3**(11), 35-46.

Tao, Z., Wang, Z.B, Yu, Q. (2013), "Finite element modelling of concrete filled steel stub columns under axial compression", *J. Constr. Steel Res.*, **89**, 121-131.

Tue, N.V., Küchler, M., Schenck, G. and Jürgen, R. (2004b), "Application of UHPC filled tubes in buildings and bridges", *Proceeding of International Symposium on Ultra High Performance Concrete*, Kassel, Germany, March.

Tue, N.V., Schneider, H., Simsch, G. and Schmidt, D. (2004a), "Bearing capacity of stub columns made of NSC, HSC and UHPC confined by a steel tube", *Proceeding of International Symposium on Ultra High Performance Concrete*, Kassel, Germany, March.

Xiong, D.X. (2012), "Structural behaviour of concrete filled steel tube with high strength materials", Ph.D. Dissertation, National University of Singapore, Singapore.

Yan, P.Y. and Feng, J.W. (2008), "Mechanical behavior of UHPC and UHPC filled steel tubular stub columns", *Proceeding of Second International Symposium on Ultra High Performance*

Concrete, Kassel, Germany.

Yang, X., Zohrevand, P. and Mirmiran, A. (2015), "Behavior of Ultrahigh-Performance concrete confined by steel", *J. Mater. Civil Eng.*, ASCE, **28**(10), 04016113.

Yang, Z., Fu, G.Y., Yu, C.J., Chen, B., Zhao, S.X. and Li, S.P. (2016), "Experimental behavior of circular flyash-concrete-filled steel tubular stub columns", *Steel Compos. Struct.*, **22**(4), 821-835.

Yu, Q., Tao, Z., Liu, W. and Chen, Z.B. (2010), "Analysis and calculations of steel tube confined concrete (STCC) stub columns", *J. Constr. Steel Res.,* **66**(1), 53-64.

Zohrevand, P. and Mirmiran, A. (2011), "Behavior of ultrahigh-performance concrete confined by fiber reinforced polymers", *J. Mater. Civil Eng.*, ASCE, **23**(12), 1727-1734.

CC